Human Molecular Genetics, 2008, Vol. 17, No. 2 ***170–178***
doi:10.1093/hmg/ddm294
Advance Access published on October 6, 2007

A rational mechanism for combination treatment of Huntington's disease using lithium and rapamycin

Sovan Sarkar[1], Gauri Krishna[1,2,†], Sara Imarisio[1,2,†], Shinji Saiki[1], Cahir J. O'Kane[2] and David C. Rubinsztein[1,*]

[1]Department of Medical Genetics, University of Cambridge, Cambridge Institute for Medical Research, Addenbrooke's Hospital, Hills Road, Cambridge CB2 0XY, UK and [2]Department of Genetics, University of Cambridge, Cambridge CB2 3EH, UK

Received August 29, 2007; Revised and Accepted October 3, 2007

Huntington's disease (HD) is caused by a polyglutamine expansion mutation in the huntingtin protein that confers a toxic gain-of-function and causes the protein to become aggregate-prone. Aggregate-prone proteins are cleared by macroautophagy, and upregulating this process by rapamycin, which inhibits the mammalian target of rapamycin (mTOR), attenuates their toxicity in various HD models. Recently, we demonstrated that lithium induces mTOR-independent autophagy by inhibiting inositol monophosphatase (IMPase) and reducing inositol and IP_3 levels. Here we show that glycogen synthase kinase-3β (GSK-3β), another enzyme inhibited by lithium, has opposite effects. In contrast to IMPase inhibition that enhances autophagy, GSK3β inhibition attenuates autophagy and mutant huntingtin clearance by activating mTOR. In order to counteract the autophagy inhibitory effects of mTOR activation resulting from lithium treatment, we have used the mTOR inhibitor rapamycin in combination with lithium. This combination enhances macroautophagy by mTOR-independent (IMPase inhibition by lithium) and mTOR-dependent (mTOR inhibition by rapamycin) pathways. We provide proof-of-principle for this rational combination treatment approach *in vivo* by showing greater protection against neurodegeneration in an HD fly model with TOR inhibition and lithium, or in HD flies treated with rapamycin and lithium, compared with either pathway alone.

INTRODUCTION

Huntington's disease (HD) is a devastating autosomal dominant neurodegenerative condition caused by abnormal expansions of a polyglutamine (polyQ) tract to more than 37 Qs in the huntingtin protein (1). Mutant huntingtin toxicity is thought to be exposed after a series of cleavage events, resulting in formation of an N-terminal fragment of around 150 residues containing the polyQ stretch. Indeed, HD pathogenesis is frequently modelled with such fragments, and transgenic animal models that express mutant huntingtin fragments recapitulate many of the behavioural and pathological features of disease (1,2).

The formation of intraneuronal aggregates in both the cytosol and the nucleus is a pathological hallmark of HD. The formation of aggregates or inclusions is a feature of many neurodegenerative diseases, including Parkinson's disease (PD), Alzheimer's disease and various autosomal dominant spinocerebellar ataxias caused by polyQ mutations. The aggregate-prone proteins causing HD and related diseases are thought to result in toxicity through gain-of-function mechanisms, although the large aggregates themselves may not be the most toxic species (1,3).

One possible approach to treating such disease may be to enhance degradation of the mutant proteins. This can be achieved by upregulating macroautophagy (which we will call autophagy) (4). Autophagy is initiated when cells form a double-layered vesicle around a portion of cytoplasm, called an autophagosome. Autophagosomes ultimately fuse with lysosomes where their contents are degraded (4).

*To whom correspondence should be addressed. Tel: +44 1223762608; Fax: +44 1223331206; Email: dcr1000@cam.ac.uk
†Joint second authors.

Autophagy can clear a wide range of intra-cytosolic aggregate-prone proteins associated with disease including mutant huntingtin (both fragments and full-length), mutant tau causing fronto-temporal dementias, mutant α-synucleins (A53T and A30P mutations) causing forms of PD and the protein causing spinocerebellar ataxia type 3 (4–9). The dependence of the aggregate-prone mutant forms on autophagy for their clearance is much higher than the wild-type proteins (6,9–12).

Autophagy can be upregulated by inhibiting the mammalian target of rapamycin (mTOR) with rapamycin, which we have shown to be beneficial in *Drosophila* models of HD and other diseases, and also in a mouse model of HD (4,5,7). We recently identified an mTOR-independent pathway regulating autophagy that depends on the levels of inositol (12). One way of enhancing autophagy with this pathway is by using lithium, as one of its activities inhibits inositol monophosphatase (IMPase) and inositol transporters (12,13). Lithium is an attractive drug to consider as it has been used for decades to treat people chronically with affective disorders and is known to pass the blood–brain barrier (14). Furthermore, we had shown that anti-apoptotic properties mediated by its ability to inhibit another enzyme, glycogen synthase kinase-3β (GSK-3β), may also be beneficial in HD (15,16).

Here we show that GSK-3β also regulates autophagy. In contrast to IMPase inhibition that enhances autophagy, GSK-3β inhibition attenuates autophagy and mutant huntingtin clearance by activating mTOR. Thus, the two enzymes inhibited by lithium have independent but opposing effects on autophagy. In order to counteract the autophagy inhibitory effects of mTOR activation resulting from lithium treatment, we have used the mTOR inhibitor rapamycin in combination with lithium as a rational combination therapy and provide support for this approach in cell and *Drosophila* models of HD.

RESULTS

Inhibition of GSK-3β retards the clearance of aggregate-prone proteins

We previously showed that lithium induced autophagy and enhanced the clearance of aggregate-prone proteins, such as mutant huntingtin and α-synucleins (12). The autophagy-inducing property of lithium was attributed to inhibition of IMPase and was independent of its effect on GSK-3β. Interestingly, we observed that a specific GSK-3β inhibitor, SB216763, increased mutant huntingtin aggregation and retarded the clearance of mutant α-synucleins (12). Accordingly, we tested if GSK-3β regulated autophagy to further clarify the actions of lithium.

We first used wild-type mouse embryonic fibroblasts (MEFs) that normally express the essential autophagy gene *Atg5* (autophagy competent; $Atg5^{+/+}$) or MEFs where *Atg5* was knocked-out (autophagy-deficient; $Atg5^{-/-}$) (17). EGFP-tagged huntingtin exon 1 with 74 polyQ repeats (EGFP-HDQ74) had more mutant huntingtin aggregation/toxicity in $Atg5^{-/-}$ cells than in $Atg5^{+/+}$ cells, as this protein is degraded by autophagy (Fig. 1A) (11,18). The specific GSK-3β inhibitor SB216763 increased EGFP-HDQ74 aggregation in $Atg5^{+/+}$ cells but not in $Atg5^{-/-}$ cells, suggesting this effect was autophagy-dependent (Fig. 1A). However, SB216763 lowered EGFP-HDQ74 toxicity in both cell lines, suggesting that it mediated some autophagy-independent anti-apoptotic effects (Fig. 1A). This is likely due to upregulation of β-catenin, which we have previously implicated in this context (16). To confirm that the protective effect of SB216763 was due to an autophagy-independent pathway regulated by β-catenin, we overexpressed constitutive active β-catenin in $Atg5^{+/+}$ and $Atg5^{-/-}$ cells where it had no effect on EGFP-HDQ74 aggregation but reduced toxicity in both cell lines (Fig. 1B).

We also confirmed that SB216763 retarded the clearance of another autophagy substrate, HA-tagged A30P mutant α-synuclein, in a stable PC12 cell line as previously shown (Supplementary Material, Fig. S1A) (12). The accumulation of autophagy substrates by SB216763 was not due to proteasome impairment, as it did not affect the levels of Ub^{G76V}-EGFP (Supplementary Material, Fig. S1B), a specific proteasome substrate that accumulates upon treatment with the proteasome inhibitor, lactacystin (19). Compatible with the above data, we observed that EGFP-HDQ74 aggregation was significantly increased in the knock-out *GSK-3β* ($GSK\text{-}3\beta^{-/-}$) MEFs compared with the wild-type MEFs ($GSK\text{-}3\beta^{+/+}$) (Fig. 1C and D). As expected, β-catenin levels were increased in the $GSK\text{-}3\beta^{-/-}$ MEFs compared with the wild-type MEFs, as they are negatively regulated by GSK3β (Fig. 1C). The above data suggest that GSK-3β inhibition retards the clearance of autophagy substrates in an autophagy-dependent and β-catenin-independent manner.

GSK-3β inhibition impairs autophagosome synthesis

We next examined how GSK-3β regulates autophagy by measuring the levels of the microtubule-associated protein 1 light chain 3 (LC3). Endogenous LC3 is processed post-translationally into LC3-I, which is cytosolic. LC3-I is converted to LC3-II, which associates with autophagosome membranes (20). LC3-II levels relative to actin/tubulin, which correlate with autophagosome number per cell (20,21), were significantly reduced in COS-7 cells treated with SB216763 compared with DMSO-treated (control) cells, and also in $GSK\text{-}3\beta^{-/-}$ cells compared with $GSK\text{-}3\beta^{+/+}$ cells (Fig. 2A and B).

In order to show that the reduction of LC3-II levels was due to impaired autophagosome synthesis, we assayed LC3-II in the presence of bafilomycin A1, which increases LC3-II levels by blocking autophagosome–lysosome fusion (22). We have previously demonstrated that autophagy-inducers can further increase LC3-II levels in bafilomycin A1-treated cells, indicating that such compounds increase autophagosome formation (11,18). On the contrary, the autophagy inhibitor SB216763 significantly decreased LC3-II levels in bafilomycin A1-treated cells [using a saturating dose of bafilomycin A1 (11)], compared with bafilomycin A1 alone, suggesting that it decreased autophagosome formation (Fig. 2C).

The impairment of autophagy due to GSK-3β inhibition was not mediated by a defect in Atg5–Atg12 conjugation, as no difference in the levels of Atg5–Atg12 conjugate was observed in $GSK\text{-}3\beta^{-/-}$ and $GSK\text{-}3\beta^{+/+}$ cells (Fig. 2D).

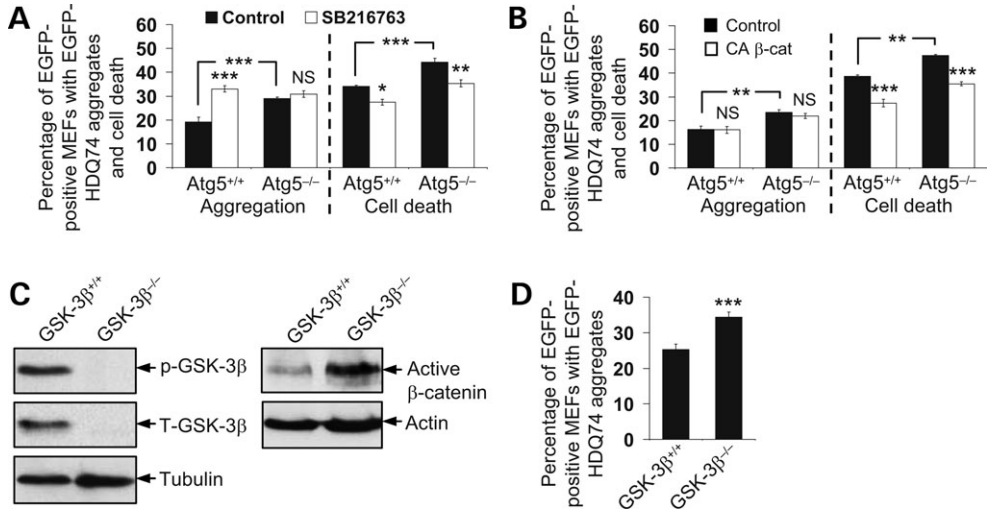

Figure 1. GSK-3β inhibition increased the aggregation of mutant huntingtin fragments independent of β-catenin. (**A**) *Atg5*$^{+/+}$ and *Atg5*$^{-/-}$ MEFs transfected with EGFP-HDQ74 for 4 h were treated with DMSO (control) or 10 μM SB216763 for 48 h. The percentage of EGFP-positive cells with EGFP-HDQ74 aggregates or cell death was assessed. SB216763 increased aggregation in *Atg5*$^{+/+}$ but not in *Atg5*$^{-/-}$ cells, whereas it reduced cell death in both the cell lines. (**B**) *Atg5*$^{+/+}$ and *Atg5*$^{-/-}$ MEFs were transfected with EGFP-HDQ74 and either pcDNA3.1 (control) or constitutive active (CA) β-catenin (1:3 ratio) for 4 h. The percentage of EGFP-positive cells with EGFP-HDQ74 aggregates or cell death was assessed at 48 h post-transfection. CA β-catenin had no effect on aggregation, whereas it reduced cell death in both the cell lines. (**C**) *GSK-3β*$^{+/+}$ and *GSK-3β*$^{-/-}$ MEFs were analysed at 24 h for phospho- and total GSK-3β, and active β-catenin levels, by immunoblotting with anti-phospho- and anti-total GSK-3β and anti-active β-catenin antibodies. Active β-catenin levels were increased in *GSK-3β*$^{-/-}$ cells compared with *GSK-3β*$^{+/+}$ cells. (**D**) The percentage of EGFP-positive cells with EGFP-HDQ74 aggregates in *GSK-3β*$^{+/+}$ and *GSK-3β*$^{-/-}$ MEFs as in Figure 1A, was counted at 48 h post-transfection. *GSK-3β*$^{-/-}$ cells had more EGFP-HDQ74 aggregates than *GSK-3β*$^{+/+}$ cells. $^{***}P < 0.001$; $^{**}P < 0.01$; $^{*}P < 0.05$; NS, non-significant.

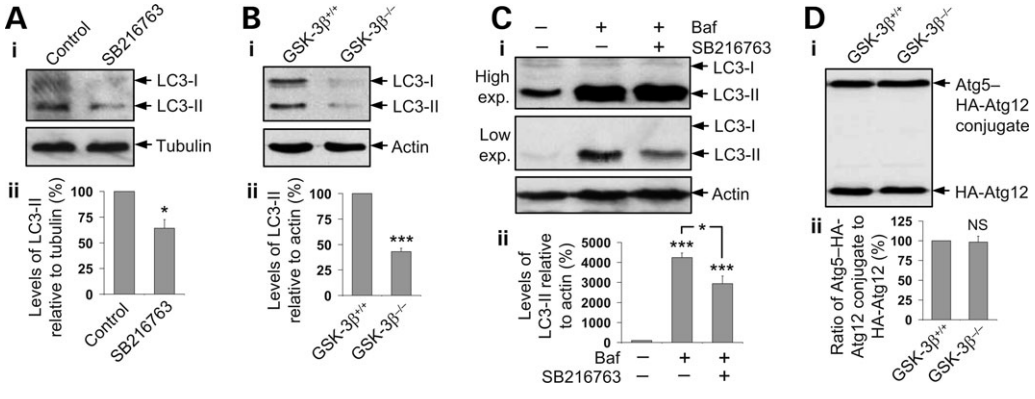

Figure 2. GSK-3β inhibition reduces LC3-II levels and inhibits autophagy. (**A**) COS-7 cells, treated with DMSO (control) or 10 μM SB216763 for 24 h, were analysed for LC3-II levels by immunoblotting with anti-LC3 antibody (i) and densitometry analysis relative to actin (ii). SB216763 reduced LC3-II levels. (**B**) *GSK-3β*$^{+/+}$ and *GSK-3β*$^{-/-}$ MEFs were analysed for LC3-II levels by immunoblotting with anti-LC3 antibody (i) at 24 h and densitometry analysis relative to actin (ii). *GSK-3β*$^{-/-}$ cells had lower LC3-II levels than *GSK-3β*$^{+/+}$ cells. (**C**) COS-7 cells, treated for 4 h with either DMSO (control) or with 400 nM bafilomycin A1 in the presence or absence of 10 μM SB216763, were analysed for LC3-II levels by immunoblotting with anti-LC3 antibody (i) and densitometry analysis relative to actin (ii). Cells were pre-treated with SB216763 for 24 h before adding bafilomycin A1. High exposure shows LC3-I levels. SB216763 reduced LC3-II levels in bafilomycin A1-treated cells, compared with bafilomycin A1 alone, suggesting an impairment in autophagosome formation. (**D**) *GSK-3β*$^{+/+}$ and *GSK-3β*$^{-/-}$ MEFs, transfected with Atg5 and HA-Atg12 constructs (1:1 ratio) for 4 h, were analysed for Atg5–HA-Atg12 conjugation at 24 h post-transfection by immunoblotting with anti-HA antibody (i) and densitometry analysis relative to actin (ii). Atg5–Atg12 conjugation was not affected in *GSK-3β*$^{-/-}$ and *GSK-3β*$^{+/+}$ cells. $^{***}P < 0.001$; $^{*}P < 0.05$; NS, non-significant.

Constitutively active GSK-3β enhances the clearance of aggregate-prone proteins by autophagy

We next overexpressed constitutively active (CA) GSK-3β in COS-7 cells, where it reduced EGFP-HDQ74 aggregation most likely by enhancing autophagy, but increased toxicity by facilitating β-catenin degradation (Fig. 3A). CA GSK-3β also reduced EGFP-HDQ74 aggregation in *Atg5*$^{+/+}$ cells, but not in *Atg5*$^{-/-}$ cells, suggesting that this effect was autophagy-dependent (Fig. 3B). Furthermore, overexpression of CA GSK-3β in *GSK-3β*$^{-/-}$ cells reduced EGFP-HDQ74 aggregation, compared with empty vector transfected *GSK-3β*$^{-/-}$ cells (Fig. 3C). The reduced aggregate level in *GSK-3β*$^{-/-}$ cells transfected with CA GSK-3β was similar to that in *GSK-3β*$^{+/+}$ cells transfected with empty vector, showing that the increased aggregation in *GSK-3β*$^{-/-}$ cells was specifically due to loss of GSK-3β (Fig. 3C). CA GSK-3β also facilitated the clearance of EGFP-tagged A53T α-synuclein mutant in a stable inducible HeLa cell line (Fig. 3D).

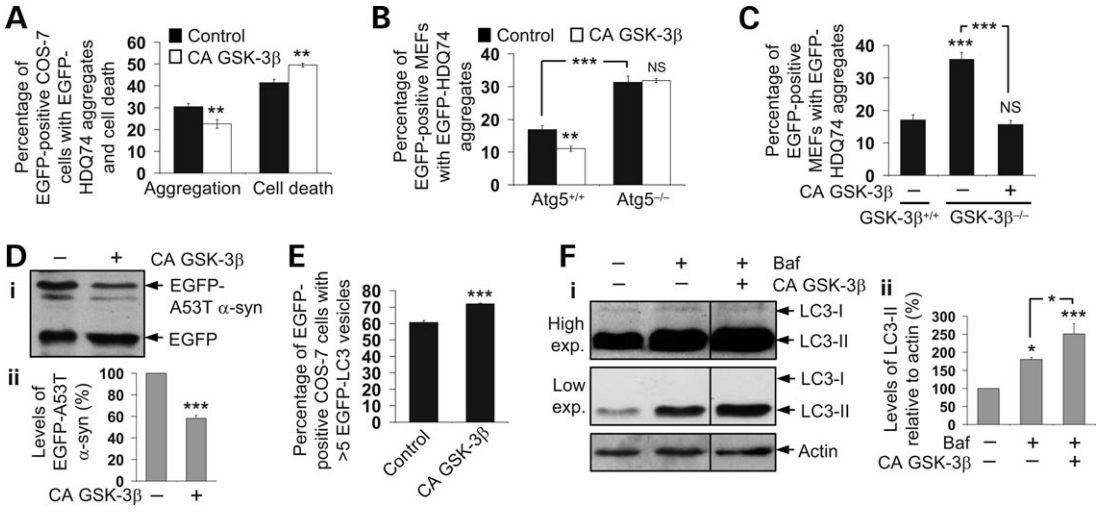

Figure 3. Constitutive active GSK-3β enhances the clearance of aggregate-prone proteins by inducing autophagy. (**A**) COS-7 cells transfected with EGFP-HDQ74 and either pcDNA3.1 (control) or CA GSK-3β (1:3 ratio) for 4 h were assessed for the percentage of EGFP-positive cells with EGFP-HDQ74 aggregates or cell death at 48 h post-transfection. CA GSK-3β reduced aggregates but increased cell death. (**B**) $Atg5^{+/+}$ and $Atg5^{-/-}$ MEFs, transfected with EGFP-HDQ74 and either pcDNA3.1 (control) or CA GSK-3β (1:3 ratio) for 4 h, were assessed for the percentage of EGFP-positive cells with EGFP-HDQ74 aggregates at 48 h post-transfection. CA GSK-3β reduced aggregation in $Atg5^{+/+}$ but not in $Atg5^{-/-}$ cells. (**C**) $GSK\text{-}3\beta^{+/+}$ MEFs transfected with EGFP-HDQ74 and pcDNA3.1 (control), or $GSK\text{-}3\beta^{-/-}$ MEFs transfected with EGFP-HDQ74 and either pcDNA3.1 (control) or CA GSK-3β (1:3 ratio) for 4 h, were assessed for the percentage of EGFP-positive cells with EGFP-HDQ74 aggregates at 48 h post-transfection. Aggregation was increased in $GSK\text{-}3\beta^{-/-}$ cells compared with $GSK\text{-}3\beta^{+/+}$ cells, and overexpression of CA GSK-3β in $GSK\text{-}3\beta^{-/-}$ cells reduced aggregate levels to levels similar to those in $GSK\text{-}3\beta^{+/+}$ cells transfected with empty vector. (**D**) Stable inducible HeLa cells expressing EGFP-A53T α-synuclein were induced with 1 μg/ml doxycycline for 48 h, and transgene expression was switched off (by removing doxycycline) for 48 h. Cells were transfected with EGFP and either pcDNA3.1 (control) or CA GSK-3β (1:3 ratio) for 4 h during switch-off period. Clearance of EGFP-A53T α-synuclein was analysed by immunoblotting with anti-EGFP antibody (i) and densitometry analysis relative to EGFP (ii). CA GSK-3β enhanced the clearance of A53T α-synuclein. (**E**) COS-7 cells, transfected with EGFP-LC3 and either pcDNA3.1 (control) or CA GSK-3β (1:3 ratio) for 4 h, were analysed for the percentage of EGFP-positive cells with more than five EGFP-LC3 vesicles at 24 h post-transfection. CA GSK-3β increased the proportion of cells with EGFP-LC3 vesicles. (**F**) COS-7 cells, transfected with pcDNA3.1 (control) or CA GSK-3β for 4 h and treated with DMSO or 400 nM bafilomycin A1 in the last 4 h of 24 h post-transfection period, were analysed for LC3-II levels by immunoblotting with anti-LC3 antibody (i) and densitometry analysis relative to actin (ii). High exposure shows LC3-I levels. CA GSK-3β increased LC3-II levels in bafilomycin A1-treated cells, compared with bafilomycin A1 alone, suggesting an increase in autophagosome formation. $^{***}P < 0.001$; $^{**}P < 0.01$; $^{*}P < 0.05$; NS, non-significant.

We next assessed the effect of CA GSK-3β on autophagy by transfecting COS-7 cells with EGFP-LC3, which localizes only to autophagic membranes but not to other membrane structures (20). Overexpression of CA GSK-3β increased autophagosome numbers, as it increased the proportion of cells with EGFP-LC3 vesicles (Fig. 3E). CA GSK-3β significantly increased LC3-II levels in the presence of bafilomycin A1, compared with bafilomycin A1 alone, suggesting that the increased autophagosomes induced by CA GSK-3β are upstream of autophagosome–lysosome fusion, at the level of autophagosome formation (Fig. 3F).

Inhibition of inositol pathway by lithium can induce autophagy independently of GSK-3β-dependent mTOR activation

To further investigate how GSK-3β regulates autophagy, we confirmed a recent study that showed that GSK-3β inhibits mTOR by phosphorylating the tuberous sclerosis complex (TSC) protein TSC2 (23). Indeed, we found mTOR activation in $GSK\text{-}3\beta^{-/-}$ MEFs, as there was increased phosphorylation of the mTOR substrate, ribosomal S6 protein kinase (S6K1, also known as p70S6K) in $GSK\text{-}3\beta^{-/-}$ cells, compared with $GSK\text{-}3\beta^{+/+}$ cells (Fig. 4A).

Lithium increased p70S6K phosphorylation in $GSK\text{-}3\beta^{+/+}$, but not in $GSK\text{-}3\beta^{-/-}$ cells (Fig. 4B). However, it reduced EGFP-HDQ74 aggregation in both the cell lines (Fig. 4C). This validated our earlier finding that lithium induces autophagy via GSK-3β- and mTOR-independent pathway regulated by inositol signaling (12). Indeed, the specific IMPase inhibitor, L-690,330, which lowers cellular inositol levels (12), had no effect on p70S6K phosphorylation, yet reduced EGFP-HDQ74 aggregation in both $GSK\text{-}3\beta^{+/+}$ and $GSK\text{-}3\beta^{-/-}$ cell lines (Fig. 4B and C), further confirming our previous assertions that autophagy regulation by the inositol pathway is independent of, or downstream of, mTOR. Rapamycin inhibited mTOR and reduced EGFP-HDQ74 aggregation in both $GSK\text{-}3\beta^{+/+}$ and $GSK\text{-}3\beta^{-/-}$ cell lines, as mTOR is downstream of GSK-3β (Fig. 4B and C). These data confirm that inositol-lowering agents such as lithium or L-690,330 could induce autophagy in spite of activated mTOR (in $GSK\text{-}3\beta^{-/-}$ cells), and these pathways are independent of each other.

Lithium and rapamycin exert additive protective effect against neurodegeneration in HD *Drosophila* model

We previously demonstrated in cell culture that lithium and rapamycin additively protect against mutant huntingtin aggregation/toxicity and enhance the clearance of soluble mutant protein, compared with either drug on its own (12). Here we further confirmed that this effect was due to the enhanced autophagic activity of the combinatorial treatment, which

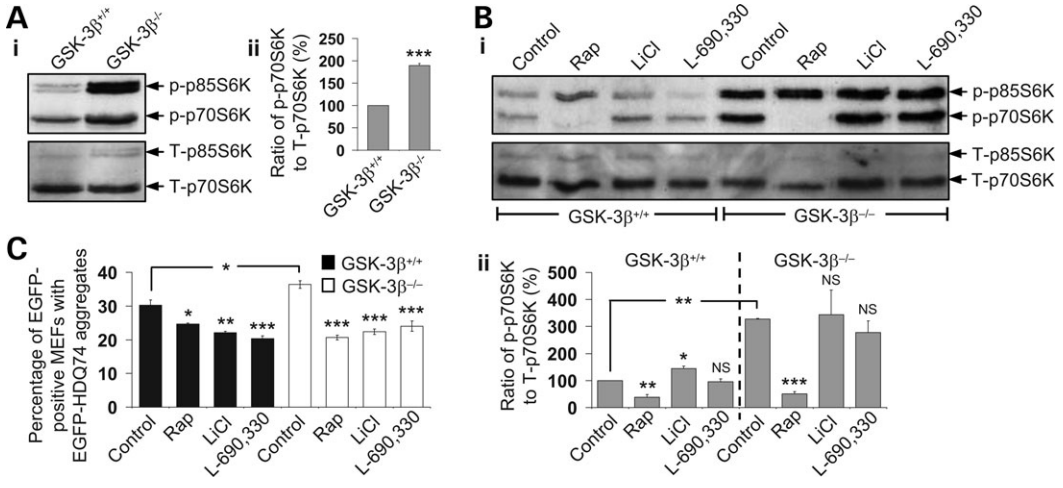

Figure 4. IMPase and mTOR inhibitors reduce mutant huntingtin aggregates in autophagy-impaired *GSK-3β*$^{-/-}$ cells where mTOR is activated. (**A**) *GSK-3β*$^{+/+}$ and *GSK-3β*$^{-/-}$ MEFs were analysed at 24 h after seeding for mTOR activity by immunoblotting with anti-phospho-p70S6K antibody (i) and densitometry analysis relative to total p70S6K (ii). The activity of mTOR (judged by the phosphorylation of its substrate p70S6K) was increased in *GSK-3β*$^{-/-}$ cells compared with *GSK-3β*$^{+/+}$ cells. (**B**) *GSK-3β*$^{+/+}$ and *GSK-3β*$^{-/-}$ MEFs, treated with or without 0.2 μM rapamycin (rap), 10 mM LiCl or 100 μM L-690,330 for 24 h, were analysed for mTOR activity by immunoblotting with anti-phospho-p70S6K antibody (i) and densitometry analysis relative to total p70S6K (ii). Rapamycin reduced p70S6K phosphorylation in *GSK-3β*$^{+/+}$ and *GSK-3β*$^{-/-}$ cell lines, where L-690,330 had no effect. LiCl increased p70S6K phosphorylation in *GSK-3β*$^{+/+}$ but not in *GSK-3β*$^{-/-}$ cells. (**C**) The percentage of EGFP-positive cells with EGFP-HDQ74 aggregates in *GSK-3β*$^{+/+}$ and *GSK-3β*$^{-/-}$ MEFs as in Figure 1D, treated with or without 0.2 μM rapamycin, 10 mM LiCl or 100 μM L-690,330 for 48 h, was assessed. Rapamycin, LiCl and L-690,330 reduced aggregation in both *GSK-3β*$^{+/+}$ and *GSK-3β*$^{-/-}$ cell lines. $^{***}P < 0.001$; $^{**}P < 0.01$; $^{*}P < 0.05$; NS, non-significant.

resulted in increased numbers of autophagosomes, as assessed by increases in EGFP-LC3 vesicles or LC3-II levels (Fig. 5A and B), compared with either lithium or rapamycin alone at saturating doses (12). We next tested the effect of this combinatorial treatment on mTOR activity. Although lithium increased mTOR activity by inhibiting GSK-3β, as assessed by the phosphorylation of p70S6K, rapamycin completely inhibited mTOR activity as seen by the absence of any p70S6K phosphorylation (Fig. 5C). Treatment with both lithium and rapamycin had a similar effect on mTOR as seen with rapamycin alone (Fig. 5C). Thus, the enhanced autophagic activity seen with the combinatorial treatment was due to mTOR-independent (IMPase inhibition by lithium) and mTOR-dependent (mTOR inhibition by rapamycin) pathways.

We next performed combinatorial treatment with lithium and rapamycin in a *Drosophila* model of HD expressing the first 171 residues of mutant huntingtin with 120 polyQ repeats in photoreceptors (24). The compound eyes in flies consist of several hundred ommatidia, each containing eight photoreceptor neurons with light-gathering parts called rhabdomeres, seven of which can be visualized using the pseudopupil technique (15). This method assesses the number of visible rhabdomeres by light microscopy and has been widely used to quantify the toxicity of proteins with long polyQs in the fly eye (5,7,15,18,24,25). The number of visible rhabdomeres in each ommatidium decreases over time in the mutant *Drosophila* that express mutant huntingtin with 120 polyQ repeats in photoreceptors, compared with the wild-type flies or transgenic flies expressing otherwise identical huntingtin with 23 polyQ (wild-type) repeats (where there is no degeneration). Lithium or rapamycin by themselves protected against neurodegeneration in *Drosophila* that expressed mutant huntingtin, compared with flies treated with the vehicle (DMSO) (7,15) (Fig. 5D and E). Combinatorial treatment with both these compounds exerted a significantly greater protective effect than either compound alone at 3 and 6 days post-eclosion (Fig. 5D and E).

Lithium and *Tor* mutant allele exert additive protective effect against neurodegeneration in HD *Drosophila* model

In order to confirm this effect further, we used a *Drosophila* heterozygous for a null allele of *Drosophila* TOR, *Tor*$^{\Delta P}$ (26). Lithium treatment of heterozygous *Tor*$^{\Delta P}$ flies carrying the HD mutation resulted in significantly greater protection against neurodegeneration, compared with the effect of heterozygous *Tor*$^{\Delta P}$ alone or lithium treatment at 6 days post-eclosion (Fig. 5G). The heterozygous *Tor*$^{\Delta P}$ mutation protected against neurodegeneration in flies carrying the HD mutation at 3 but not 6 days post-eclosion (Fig. 5F and G), as rapamycin at micromolar concentrations lowers TOR activity more efficiently than the 50% reduction expected in heterozygous *Tor*$^{\Delta P}$ (26). These data further confirmed the combination effect seen with two independent autophagy-inducing pathways.

DISCUSSION

Here we have reported that GSK-3β is a positive regulator of autophagy, as it inhibits mTOR. Thus, the targets of lithium, IMPase and GSK-3β, have two opposing effects on autophagy. Lithium enhances autophagy by inhibiting IMPase and reducing the levels of inositol and myo-inositol-1,4,5-triphosphate (IP_3), and suppresses autophagy by inhibiting GSK-3β (Fig. 6A). These conflicting effects may explain the equivocal effects of this drug in an HD mouse model (27).

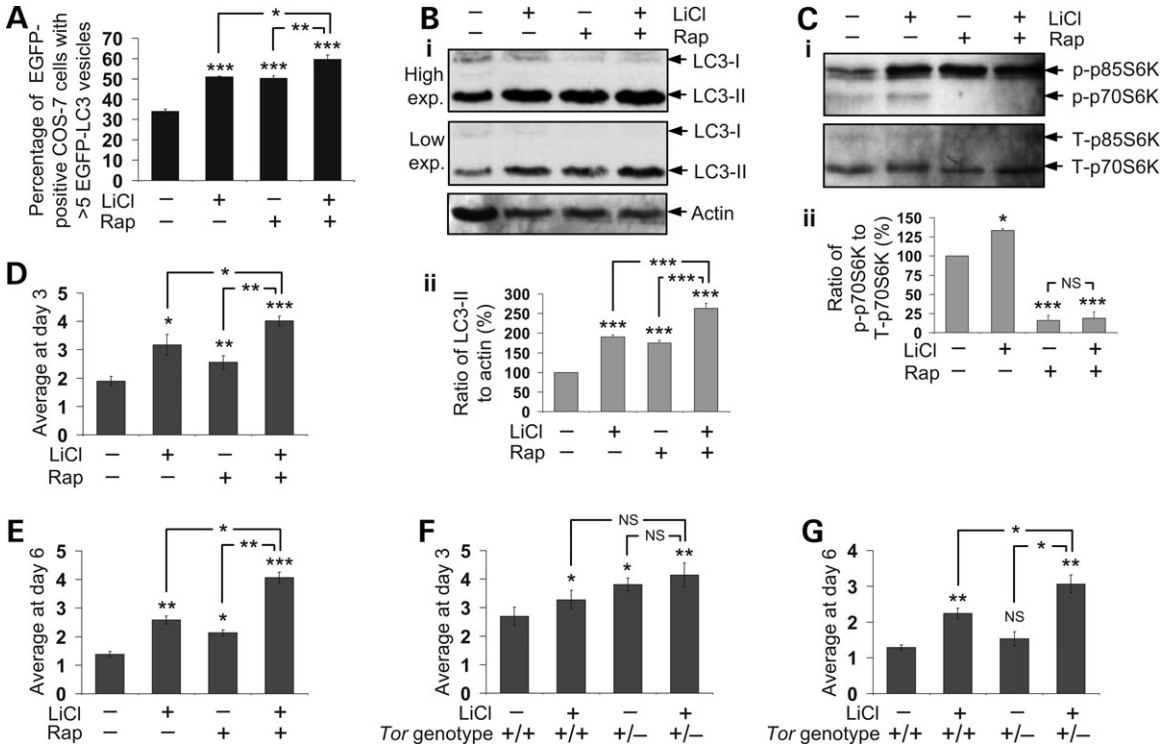

Figure 5. Lithium and rapamycin have additive autophagy-inducing effects in cells and in rescuing polyQ-mediated toxicity in *Drosophila*. (**A**) COS-7 cells transfected with EGFP-LC3 for 4 h and treated with or without 10 mM LiCl, 0.2 μM rapamycin or both were analysed for the percentage of EGFP-positive cells with more than five EGFP-LC3 vesicles at 24 h post-transfection. Combination treatment with LiCl and rapamycin led to greater proportions of cells with more than five EGFP-LC3 vesicles, compared with either of the compounds alone. (**B**) COS-7 cells treated with or without 10 mM LiCl, 0.2 μM rapamycin or both for 24 h were analysed for autophagy by immunoblotting with anti-LC3 antibody (i) and densitometry analysis relative to actin (ii). Combination treatment with LiCl and rapamycin led to higher levels of LC3-II, compared with either treatment alone. (**C**) COS-7 cells treated with or without 10 mM LiCl, 0.2 μM rapamycin or both for 24 h were analysed for mTOR activity by immunoblotting with anti-phospho-p70S6K antibody (i) and densitometry analysis relative to total p70S6K (ii). Whereas LiCl alone increases p70S6K phosphorylation, treatment with both lithium and rapamycin inhibited mTOR activity (like rapamycin alone). (**D** and **E**) Pseudopupil analysis of *gmr-httQ120* flies reared in the presence or absence of 4.2 mM lithium, 2 μM rapamycin and combination of both, 3 (D) and 6 (E) days post-eclosion. Paired *t*-test, $n = 6$. Combination treatment with LiCl and rapamycin exerted greater protection against neurodegeneration, compared with the protective effects of either compounds alone. (**F** and **G**) Pseudopupil analysis of flies carrying *gmr-httQ120* either in a Tor^{+} (+/+) or with heterozygous $Tor^{\Delta P}$/+ (+/−) background in the presence or absence 4.2 mM lithium. Rhabdomeres were scored 3 (F) and 6 (G) days post-eclosion. Experiment was done as in (D and E). Genotypes: *y w; gmr-httQ120/+* (+/+), *y w; gmr-httQ120/*$Tor^{\Delta P}$ (+/−). The heterozygous $Tor^{\Delta P}$ mutation is expected to have a 50% loss of *Drosophila* TOR activity in contrast to the more severe impairment of TOR activity by rapamycin. Thus, $Tor^{\Delta P}$ mutation protected against neurodegeneration in flies with the HD mutation at 3 but not 6 days post-eclosion. The heterozygous $Tor^{\Delta P}$ mutation and lithium showed greater protection at 6 days post-eclosion, compared with the mutation or lithium alone. $^{***}P < 0.001$; $^{**}P < 0.01$; $^{*}P < 0.05$; NS, non-significant.

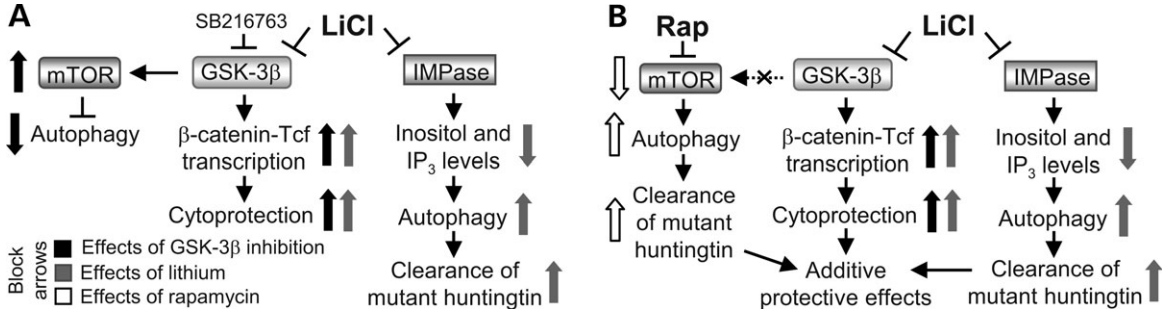

Figure 6. Schematic representation of the combinatorial treatment strategy for HD. (**A**) GSK-3β inhibition (by lithium or SB216763) negatively regulates autophagy by activating mTOR, but is cytoprotective by enhancing β-catenin-Tcf transcription. The IMPase-inhibitory property of lithium induces mTOR-independent autophagy by lowering inositol and IP_3 levels, thereby facilitating mutant huntingtin clearance. (**B**) Rapamycin induces autophagy by inhibiting mTOR, which is downstream of GSK-3β, thereby alleviating the effect of GSK-3β on mTOR. Combination treatment of lithium and rapamycin facilitates greater clearance of mutant huntingtin by induction of autophagy through mTOR-independent (lithium) and mTOR-dependent (rapamycin) pathways, compared with either treatment alone. The enhanced autophagy due to combinatorial treatment, coupled with the anti-apoptotic effects of increased β-catenin-Tcf transcription by lithium, may be therapeutically relevant in HD.

We have shown that the undesirable effect of GSK-3β inhibition on autophagy via mTOR activation can be abrogated by simultaneously treating with rapamycin (Fig. 6B). Accordingly, lithium and rapamycin exert additive protective effects on autophagic clearance of mutant huntingtin fragments (12). This approach is effective as rapamycin inhibits mTOR directly and downstream of the GSK-3β effect. The elucidation of the mechanism by which GSK-3β inhibition blocks autophagy provides a rational basis for combination treatment of diseases such as HD with lithium and rapamycin. Inhibition of the mTOR and/or inositol pathways regulates autophagy in both neuronal and non-neuronal cell lines (12). Our data provide proof-of-principle for this approach using *Drosophila* models, which allow one to establish the saturating doses of rapamycin experimentally, and confirm certain pharmacological effects genetically. Note that both lithium and rapamycin can cross the blood–brain barrier and are used to treat chronic diseases in humans over decades.

We believe that the combination of rapamycin and lithium is attractive as it allows one to maximize the benefits of autophagy upregulation by mTOR-dependent and mTOR-independent routes, which are additive. An alternative strategy would be to use lower doses of both the compounds in combination, which may also lessen drug-specific side effects. Lithium also has likely anti-apoptotic beneficial effects in HD models via the β-catenin-TCF pathway (15,16) (Fig. 6B). Thus, the lithium and rapamycin combination enhances autophagy via two distinct pathways and also protects against cell death/apoptosis.

MATERIALS AND METHODS

Plasmids

HD gene exon 1 fragment with 74 polyQ repeats in pEGFP-C1 (Clontech) (EGFP-HDQ74) construct was characterized previously (28). We used constructs encoding CA GSK-3β (kind gift from J.-M. Gallo, Institute of Psychiatry, London), CA β-catenin (kind gift from M. Bienz, Laboratory of Molecular Biology, Cambridge), EGFP-LC3 (kind gift from T. Yoshimori, Japanese National Institute of Genetics), Atg5 and HA-Atg12 (kind gifts from N. Mizushima, Tokyo Metropolitan Institute of Medical Science).

Mammalian cell culture and transfection

African green monkey kidney cells (COS-7), wild-type Atg5 ($Atg5^{+/+}$) and Atg5-deficient ($Atg5^{-/-}$) MEFs (17) (kind gift from N. Mizushima) and wild-type GSK-3β ($GSK\text{-}3\beta^{+/+}$) and GSK-3β-deficient ($GSK\text{-}3\beta^{-/-}$) MEFs (29) (kind gift from J. Woodgett, Samuel Lunenfeld Research Institute, Toronto) were maintained in DMEM (Sigma) supplemented with 10% FBS (Sigma), 100 U/ml penicillin/streptomycin (Sigma) and 2 mM L-glutamine (Sigma) at 37°C, 5% CO_2. HeLa cells stably expressing Ub^{G76V}-EGFP reporter (19) (kind gift from N.P. Dantuma, Karolinska Institutet, Stockholm) were grown in the same media used for COS-7 cells supplemented with 0.5 mg/ml G418 (GIBCO).

Inducible PC12 stable cell line expressing HA-tagged A30P α-synuclein mutant, previously characterized (6), was maintained using 75 μg/ml hygromycin B (Calbiochem) in DMEM with 10% horse serum (Sigma), 5% FBS, 100 U/ml penicillin/streptomycin, 2 mM L-glutamine and 100 μg/ml G418 at 37°C, 10% CO_2.

Cells were transfected with the constructs for 4 h using Lipofectamine or Lipofectamine 2000 reagent (Invitrogen) according to manufacturer's protocol, fixed with 4% paraformaldehyde (Sigma) after 48 h (EGFP-HDQ74) or 24 h (EGFP-LC3) post-transfection and mounted in citifluor (Citifluor Ltd) containing 4′,6-diamidino-2-phenylindole (DAPI; 3 μg/ml; Sigma-Aldrich).

Generation of stable HeLa cell line expressing EGFP-A53T α-synuclein

EGFP-tagged full-length A53T α-synuclein was cloned into a pTRE2hyg vector. Inducible HeLa cell lines stably expressing EGFP-A53T α-synuclein were established using a HeLa Tet-on line (Clontech) and cultured in DMEM supplemented with 10% FBS, 2 mM L-glutamine, 100 U/ml penicillin/streptomycin, 100 μg/ml G418 and 200 μg/ml hygromycin B at 37°C, 5% CO_2. The construct did not have any toxicity in this cell line.

Quantification of mutant huntingtin aggregates and cell death

The percentage of EGFP-positive cells with EGFP-HDQ74 aggregates or apoptotic morphology (cell death) was counted as previously described (11,12,18).

Autophagy methods

Assessment of autophagy by EGFP-LC3 vesicles. The percentage of EGFP-positive cells with more than five EGFP-LC3 vesicles was counted, as previously described (12).

Assessment of autophagy by LC3-II levels. LC3-II levels, which directly correlate with autophagosome numbers (20,21), is detected with anti-LC3 antibody (NB100-2220, Novus Biologicals) and densitometry analysis relative to actin/tubulin (30). To see if accumulation of LC3-II is due to increased autophagosome formation or impaired autophagosome–lysosome fusion, LC3-II is assessed in the presence of bafilomycin A1, that blocks autophagosome–lysosome fusion (22), as shown previously (11,18).

Reagents

Compounds used in cell culture were 10 μM SB216763 (Tocris), 10 mM LiCl (Sigma-Aldrich), 0.2 μM Rapamycin (Sigma-Aldrich), 100 μM L-690,330 (Tocris), 400 nM Bafilomycin A1 (Sigma-Aldrich), 10 μM Lactacystin (Biomol).

Microscopy

Transfected cells were analysed for EGFP-HDQ74 aggregation/cell death or EGFP-LC3 vesicles using Nikon Eclipse E600 fluorescence microscope (plan-apo 60×/1.4 oil immersion lens at room temperature) (Nikon, Inc.).

Clearance of mutant α-synucleins

Stable inducible PC12 or HeLa cell lines expressing HA-A30P or EGFP-A53T α-synuclein were induced with 1 μg/ml doxycycline (Sigma) for 48 h, respectively. The transgene expression was switched off by removing doxycycline from medium (6). Cells were treated with or without compounds, or transfected with plasmids, for time-points as indicated in experiments. Clearance of A30P or A53T α-synuclein was measured by immunoblotting with antibody against HA or EGFP, respectively, and densitometry analysis relative to actin.

Western blot

Cell pellets were lysed on ice in Laemmli buffer (62.5 mM Tris–HCl pH 6.8, 5% β-mercaptoethanol, 10% glycerol and 0.01% bromophenol blue) for 30 min in the presence of protease inhibitors (Roche Diagnostics). Primary antibodies include anti-EGFP (8362-1, Clontech), anti-HA (12CA5, Covance), anti-LC3 (NB100-2220, Novus Biologicals), anti-p70 S6 kinase (9202, Cell Signaling Technology), anti anti-phospho-p70 S6 kinase (Thr389) (9206, Cell Signaling Technology), anti-GSK-3β (9315, Cell Signaling Technology), anti anti-phospho-GSK-3β (Ser9) (9336, Cell Signaling Technology), anti-active β-catenin (05-665, Upstate Cell Signaling Solutions), anti-actin (A2066, Sigma) and anti-tubulin (Clone DM 1A, Sigma). Blots were probed with anti-mouse or anti-rabbit IgG-HRP and visualized using ECL detection kit (Amersham).

Drosophila stocks

To test the effect of *Tor* mutants, virgins carrying *y w; gmr-httQ120* (24) were crossed with either *y w; To$^{\Delta P}$ Pwa40A/CyO* (26) or with isogenic *w^{1118}* males line as control (31). Flies were reared at 25°C on instant fly food (Philip Harris Ltd) containing the appropriate drug. All crosses were done at the same time and under the same conditions.

Drug treatments in *Drosophila*

The above crosses were reared on 4.2 mM lithium (Calbiochem) and 2 μM rapamycin (L.C. Laboratories) mixed with instant fly food. Control flies grown in the absence of drug were fed with instant fly food with 0.02% DMSO (Sigma). Combination treatments were done using 4.2 mM lithium and 2 μM rapamycin. Flies were treated during both larval and adult stages.

Drosophila pseudopupil analysis

Pseudopupil analysis was performed as described before (15). Mann-Whitney *U* tests were used to compare raw data, and paired *t*-tests were used to compare averages based on multiple experiments. In each experiment, values for each condition or genotype were based on 10 eyes and 15 ommatidia per eye. Control was arbitrarily set at 100% to enable comparison of multiple independent experiments. STATVIEW v4.53 was used for statistical analysis.

Statistical analysis

The *P*-values for assessing EGFP-HDQ74 aggregation/cell death and EGFP-LC3 vesicles were determined by unconditional logistical regression analysis, using the general log-linear analysis option of SPSS 9 software (SPSS, Chicago, IL, USA). Densitometry analysis on immunoblots was done by Scion Image Beta 4.02 software (Scion Corporation) from three independent experiments, and *P*-values were determined by factorial ANOVA test using STATVIEW v4.53 (Abacus Concepts), where control was set to 100%. The *y*-axis values are shown in percentage (%) and error bars denote standard error of mean. $^{***}P < 0.001$; $^{**}P < 0.01$; $^{*}P < 0.05$; NS, non-significant.

SUPPLEMENTARY MATERIAL

Supplementary Material is available at HMG Online.

ACKNOWLEDGEMENTS

We thank T. Yoshimori for EGFP-LC3 construct, N. Mizushima for wild-type Atg5 and HA-Atg12 constructs and *Atg5$^{+/+}$* and *Atg5$^{-/-}$* MEFs, J.R. Woodgett for *GSK-3β$^{+/+}$* and *GSK-3β$^{-/-}$* MEFs, J.-M. Gallo for constitutive active GSK-3β construct, M. Bienz for constitutive active β-catenin construct, N.P. Dantuma for Ub^{G76V}-EGFP HeLa stable cells, G.R. Jackson for the *gmr-httQ120* flies, Bloomington Drosophila Stock Center for *Tor$^{\Delta P}$* flies, J.E. Davies, B. Ravikumar and V.I. Korolchuk for helpful comments on the manuscript.

Conflict of Interest statement. The authors declare no conflict of interest.

FUNDING

This study was funded by Hughes Hall Research Fellowship (Sov.S.), Eli Lilly Pergolide Fellowship (Shi.S.), Wellcome Trust Senior Fellowship in Clinical Science (D.C.R.), an M.R.C. Programme Grant and E.U. Framework VI (EUROSCA). Funding to pay the open access publication charge was provided by the Wellcome Trust.

REFERENCES

1. Rubinsztein, D.C. (2002) Lessons from animal models of Huntington's disease. *Trends Genet.*, **18**, 202–209.
2. Kuhn, A., Goldstein, D.R., Hodges, A., Strand, A.D., Sengstag, T., Kooperberg, C., Becanovic, K., Pouladi, M.A., Sathasivam, K., Cha, J.H. *et al.* (2007) Mutant huntingtin's effects on striatal gene expression in mice recapitulate changes observed in human Huntington's disease brain and do not differ with mutant huntingtin length or wild-type huntingtin dosage. *Hum. Mol. Genet.*, **16**, 1845–1861.
3. Ross, C.A. and Poirier, M.A. (2005) What is the role of protein aggregation in neurodegeneration?. *Nat. Rev. Mol. Cell Biol.*, **6**, 891–898.
4. Rubinsztein, D.C., Gestwicki, J.E., Murphy, L.O. and Klionsky, D.J. (2007) Potential therapeutic applications of autophagy. *Nat. Rev. Drug Discov.*, **6**, 304–312.
5. Berger, Z., Ravikumar, B., Menzies, F.M., Oroz, L.G., Underwood, B.R., Pangalos, M.N., Schmitt, I., Wullner, U., Evert, B.O., O'Kane, C.J. *et al.* (2006) Rapamycin alleviates toxicity of different aggregate-prone proteins. *Hum. Mol. Genet.*, **15**, 433–442.

6. Webb, J.L., Ravikumar, B., Atkins, J., Skepper, J.N. and Rubinsztein, D.C. (2003) Alpha-synuclein is degraded by both autophagy and the proteasome. *J. Biol. Chem.*, **278**, 25009–25013.
7. Ravikumar, B., Vacher, C., Berger, Z., Davies, J.E., Luo, S., Oroz, L.G., Scaravilli, F., Easton, D.F., Duden, R., O'Kane, C.J. *et al.* (2004) Inhibition of mTOR induces autophagy and reduces toxicity of polyglutamine expansions in fly and mouse models of Huntington disease. *Nat. Genet.*, **36**, 585–595.
8. Shibata, M., Lu, T., Furuya, T., Degterev, A., Mizushima, N., Yoshimori, T., MacDonald, M., Yankner, B. and Yuan, J. (2006) Regulation of intracellular accumulation of mutant Huntingtin by Beclin 1. *J. Biol. Chem.*, **281**, 14474–14485.
9. Ravikumar, B., Duden, R. and Rubinsztein, D.C. (2002) Aggregate-prone proteins with polyglutamine and polyalanine expansions are degraded by autophagy. *Hum. Mol. Genet.*, **11**, 1107–1117.
10. Berrios, G.E., Wagle, A.C., Markova, I.S., Wagle, S.A., Ho, L.W., Rubinsztein, D.C., Whittaker, J., Ffrench-Constant, C., Kershaw, A., Rosser, A. *et al.* (2001) Psychiatric symptoms and CAG repeats in neurologically asymptomatic Huntington's disease gene carriers. *Psychiatry Res.*, **102**, 217–225.
11. Sarkar, S., Davies, J.E., Huang, Z., Tunnacliffe, A. and Rubinsztein, D.C. (2007) Trehalose, a novel mTOR-independent autophagy enhancer,accelerates the clearance of mutant huntingtin and alpha-synuclein. *J. Biol. Chem.*, **282**, 5641–5652.
12. Sarkar, S., Floto, R.A., Berger, Z., Imarisio, S., Cordenier, A., Pasco, M., Cook, L.J. and Rubinsztein, D.C. (2005) Lithium induces autophagy by inhibiting inositol monophosphatase. *J. Cell Biol.*, **170**, 1101–1111.
13. Phiel, C.J. and Klein, P.S. (2001) Molecular targets of lithium action. *Annu. Rev. Pharmacol. Toxicol.*, **41**, 789–813.
14. Manji, H.K. and Lenox, R.H. (1998) Lithium: a molecular transducer of mood-stabilization in the treatment of bipolar disorder. *Neuropsychopharmacology*, **19**, 161–166.
15. Berger, Z., Ttofi, E.K., Michel, C.H., Pasco, M., Tenant, S., Rubinsztein, D.C. and O'Kane, C.J. (2005) Lithium rescues toxicity of aggregate-prone proteins in *Drosophila* by perturbing Wnt pathway. *Hum. Mol. Genet.*, **14**, 3003–3011.
16. Carmichael, J., Sugars, K.L., Bao, Y.P. and Rubinsztein, D.C. (2002) Glycogen synthase kinase-3beta inhibitors prevent cellular polyglutamine toxicity caused by the Huntington's disease mutation. *J. Biol. Chem.*, **277**, 33791–33798.
17. Mizushima, N., Yamamoto, A., Hatano, M., Kobayashi, Y., Kabeya, Y., Suzuki, K., Tokuhisa, T., Ohsumi, Y. and Yoshimori, T. (2001) Dissection of autophagosome formation using Apg5-deficient mouse embryonic stem cells. *J. Cell Biol.*, **152**, 657–668.
18. Sarkar, S., Perlstein, E.O., Imarisio, S., Pineau, S., Cordenier, A., Maglathlin, R.L., Webster, J.A., Lewis, T.A., O'Kane, C.J., Schreiber, S.L. *et al.* (2007) Small molecules enhance autophagy and reduce toxicity in Huntington's disease models. *Nat. Chem. Biol.*, **3**, 331–338.
19. Dantuma, N.P., Lindsten, K., Glas, R., Jellne, M. and Masucci, M.G. (2000) Short-lived green fluorescent proteins for quantifying ubiquitin/proteasome-dependent proteolysis in living cells. *Nat. Biotechnol.*, **18**, 538–543.
20. Kabeya, Y., Mizushima, N., Ueno, T., Yamamoto, A., Kirisako, T., Noda, T., Kominami, E., Ohsumi, Y. and Yoshimori, T. (2000) LC3, a mammalian homologue of yeast Apg8p, is localized in autophagosome membranes after processing. *EMBO J.*, **19**, 5720–5728.
21. Mizushima, N. (2004) Methods for monitoring autophagy. *Int. J. Biochem. Cell Biol.*, **36**, 2491–2502.
22. Yamamoto, A., Tagawa, Y., Yoshimori, T., Moriyama, Y., Masaki, R. and Tashiro, Y. (1998) Bafilomycin A1 prevents maturation of autophagic vacuoles by inhibiting fusion between autophagosomes and lysosomes in rat hepatoma cell line, H-4-II-E cells. *Cell Struct. Funct.*, **23**, 33–42.
23. Inoki, K., Ouyang, H., Zhu, T., Lindvall, C., Wang, Y., Zhang, X., Yang, Q., Bennett, C., Harada, Y., Stankunas, K. *et al.* (2006) TSC2 integrates Wnt and energy signals via a coordinated phosphorylation by AMPK and GSK3 to regulate cell growth. *Cell*, **126**, 955–968.
24. Jackson, G.R., Salecker, I., Dong, X., Yao, X., Arnheim, N., Faber, P.W., MacDonald, M.E. and Zipursky, S.L. (1998) Polyglutamine-expanded human huntingtin transgenes induce degeneration of *Drosophila* photoreceptor neurons. *Neuron*, **21**, 633–642.
25. Marsh, J.L. and Thompson, L.M. (2006) *Drosophila* in the study of neurodegenerative disease. *Neuron*, **52**, 169–178.
26. Zhang, H., Stallock, J.P., Ng, J.C., Reinhard, C. and Neufeld, T.P. (2000) Regulation of cellular growth by the *Drosophila* target of rapamycin dTOR. *Genes Dev.*, **14**, 2712–2724.
27. Wood, N.I. and Morton, A.J. (2003) Chronic lithium chloride treatment has variable effects on motor behaviour and survival of mice transgenic for the Huntington's disease mutation. *Brain Res. Bull.*, **61**, 375–383.
28. Narain, Y., Wyttenbach, A., Rankin, J., Furlong, R.A. and Rubinsztein, D.C. (1999) A molecular investigation of true dominance in Huntington's disease. *J. Med. Genet.*, **36**, 739–746.
29. Liu, S., Yu, S., Hasegawa, Y., Lapushin, R., Xu, H.J., Woodgett, J.R., Mills, G.B. and Fang, X. (2004) Glycogen synthase kinase 3beta is a negative regulator of growth factor-induced activation of the c-Jun N-terminal kinase. *J. Biol. Chem.*, **279**, 51075–51081.
30. Mizushima, N. and Yoshimori, T. (2007) How to interpret LC3 immunoblotting. *Autophagy*, **3**.
31. Ryder, E., Blows, F., Ashburner, M., Bautista-Llacer, R., Coulson, D., Drummond, J., Webster, J., Gubb, D., Gunton, N., Johnson, G. *et al.* (2004) The DrosDel collection: a set of P-element insertions for generating custom chromosomal aberrations in *Drosophila* melanogaster. *Genetics*, **167**, 797–813.